

Augmenting Learning Components for Safety in Resource Constrained Autonomous Robots

Shreyas Ramakrishna*, Abhishek Dubey*, Matthew P Burruss*, Charles Hartsell*
Nagabhushan Mahadevan*, Saideep Nannapaneni†, Aron Laszka‡, Gabor Karsai*

*Vanderbilt University

†Wichita State University

‡University of Houston

Abstract—This paper deals with resource constrained autonomous robots commonly found in factories, hospitals, and education laboratories, which popularly use learning enabled components (LEC) to make control actions. However, these LECs do not provide any safety guarantees, and testing them is challenging. To overcome these challenges, we introduce a framework that performs confidence estimation, resource management, and supervised safety control of autonomous systems with LECs. Using this framework, we make the following contributions: (1) allow for seamless integration of safety controllers and different simplex strategies to aid the LEC, (2) introduce RL-Simplex and illustrate the use of Q-learning to learn the optimal weights for the arbitration logic of the Simplex Architecture, (3) design a system level monitor that uses the current state information and a discrete Bayesian network model learned from past data to estimate a metric, which indicates if the car will remain in the safe region, and (4) a Resource Manager which performs dynamic task offloading depending on the resource temperature and CPU utilization while continually adjusting vehicle speed to compensate for the latency overhead. We compare the speed, steering and safety performance of the different controllers and simplex strategies, and we find RL-Simplex to have 60% fewer safety violations and higher optimized speed during indoor driving ($\sim 0.40 m/s$) than the original system (using only LEC).

Index Terms—Autonomous Robots, LEC, Convolutional Neural Networks, Simplex Architecture, Reinforcement Learning.

ACRONYMS

AM Arguing Machines
CPS Cyber Physical System
CNN Convolutional Neural Network
DMA Decision Manager Actor
LD Lane Detection
LEC Learning Enabled Component
MBA Message Buffer Actor
RL Reinforcement Learning
RM Resource Manager
SS Safety Supervisor

I. INTRODUCTION

Autonomous systems are a class of systems that interact with the surrounding environment, gather information, and perform required tasks in an automated manner without human intervention. Examples can be found in various domains such as transportation (self-driving cars [1], [2], buses), manufacturing (robotic arms, service robots), agriculture, social care, and search-and-rescue disaster management (autonomous drones [3]). Techniques for training autonomous systems include

human encoded control and reinforcement learning. Reinforcement learning [4] is a powerful data-driven strategy in which the learning happens in a closed loop agent-environment interactions whereas the other techniques are associated with human involvement. In the presence of huge amounts of training data, some autonomous systems have surpassed human experts in performance, for example, the Alpha Go Zero [5]. A key framework in realizing autonomy is end-to-end (e2e) learning, which makes use of deep learning. For example, NVIDIA'S DAVE-II [1], ALVINN [2], and DeepPicar [6] use Convolutional Neural Networks (CNN) to design the controller for the autonomous system. Therefore, a combination of reinforcement learning and deep learning approaches provide a framework to transition from model-based system components to data-driven LECs.

While the use of data-driven LECs provides a paradigm shift in the ability to create adaptive systems, it also presents challenges in testing and assurance. For example, there are no established analogues to path coverage based testing mechanisms for components designed with neural networks. There has been ongoing research in designing tools for automated testing of Deep Neural Network driven systems like [7], [8], however they are limited by the exhaustive test case scenarios they support, and hence may not detect all the edge cases. In addition, existing verification tools [9], [10] have been largely limited with the type of the activation function and complexity of the neural networks that can be analyzed.

The key challenges in establishing confidence in data-driven LEC systems are (1) unknown operating contexts [11] – the environments in which the autonomous systems to be used are not completely known (e.g., search-and-rescue robots), and (2) the environments may be known but generating data is often associated with a lot of human labor and large training time, which might not be available. Presence of limited data reduces the confidence in the trained system.

Safety-critical Cyber Physical Systems (CPS) like aircrafts (Boeing 777 [12]), unmanned aerial vehicles (UAV) [13], and mission critical ground rovers [14] are augmented with Simplex Architectures [12] to increase the system assurance. This architectural pattern allows the integration of safety supervisors operating in parallel to the unverified controllers (LECs), with a decision manager to perform arbitration between the controllers. Similar to Simplex Architectures, Fridman et al.

Symbol	Description
S_R	Steering PWM value of DeepNNCar using RL-Simplex
S_L	Steering PWM value of DeepNNCar using LEC
S_S	Steering PWM value of DeepNNCar using Safety Supervisor
S_{SA}	Steering PWM value using classical Simplex Architecture
S_{AM}	Steering PWM value of DeepNNCar using AM-Simplex
T_R	Inference pipeline time of DeepNNCar using RL-Simplex
V	Current speed of DeepNNCar
V_{MAX}	Max Saturated speed during task offload
V_{SET}	Set speed computed by the RL-Simplex
W_L	Arbitration weight given to LEC controller.
W_S	Arbitration weight given to Safety Supervisor.
W_{SET}	Arbitration weights $\{W_L, W_S\}$ computed by RL-Simplex
STOP	Command from Safety Supervisor during safety violations
\hat{M}	Estimated state of the track segment
\hat{t}	Deviation of car from the track center
I	Image captured by the front facing camera

TABLE I: List of Symbols

[15] have proposed the Arguing Machine concept, which has two LECs working in parallel with a predefined threshold as the switching criteria. This architecture allows us to encode domain knowledge such as information regarding the operating environment or actions to be taken in particular operating conditions. These rules can provide constraints to the LEC and improve their operational performance.

However, the problem with these approaches is that they use fixed arbitration weights irrespective of the different operational modes and contexts of the working environment. Biswas et al. [16] have shown that mode detection is a crucial problem and data-driven anomaly detection methods should be mode and context sensitive. We hypothesize the same is true for Simplex Architectures. Another problem is that they do not provide any confidence metric that can be used to evaluate the decisions of the LEC if safety violations occur. Such diagnostic capabilities are crucial in safety-critical systems. This leads to the research question: Can we provide a middleware framework that (a) can be augmented with pre-trained LECs, which acts as an online supervisor learning from the past actions, and aggregates data from the past operation to continuously enhance its learning experience, and (b) provide a confidence metric about the safety of current actions at system level in real-time, given all the past actions?

Our Contributions: This paper presents a framework that performs supervised control of systems with LECs, provides confidence estimation for their operation, and manages its resources. The contributions discussed in this paper are: (a) an adaptive framework that allows for integration of different controllers and simplex strategies, and allows for active switching among them based on the performance of the system; (b) a reinforcement learning-based simplex (RL-Simplex) strategy that allows to succinctly learn a Q-table of optimal arbitration weights that are flexible to changing modes and contexts; (c) a system monitor which uses the current state information of the car and a Bayesian network model to estimate a metric which indicates if the car will be in the safe working region or not; and (d) a task offloading strategy that performs resource

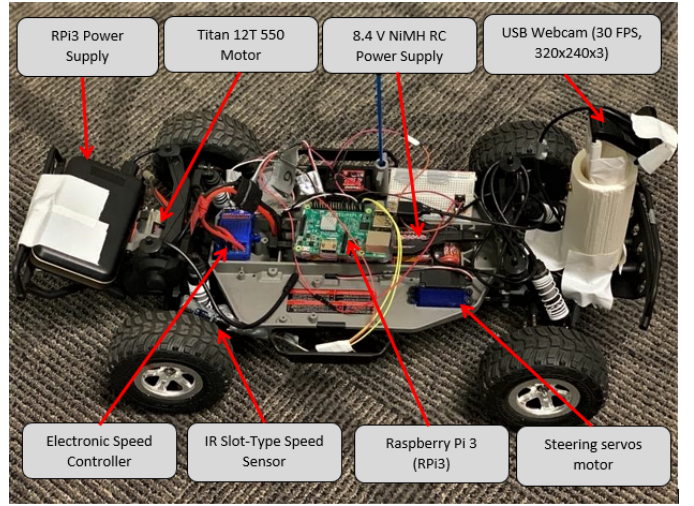


Fig. 1: DeepNNCar platform with different onboard components and sensors

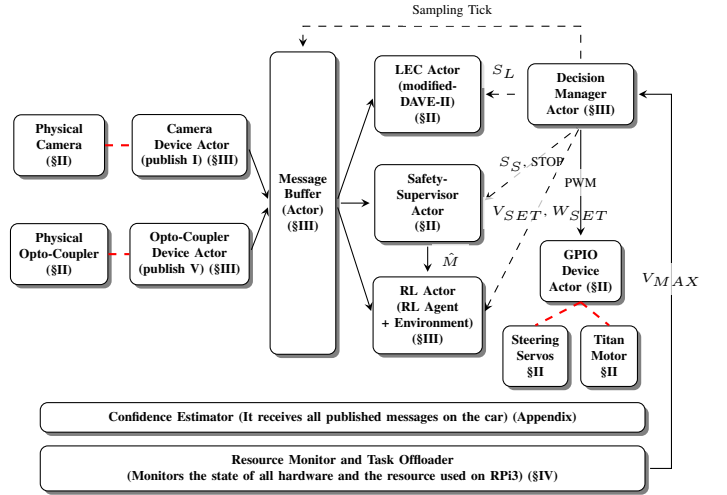


Fig. 2: A block diagram of DeepNNCar along with the different components. There are asynchronous interaction among various components and so we have used different messaging patterns. The request-reply communications are shown with dotted lines, the publish-subscribe communications are shown in solid lines, and the red dotted lines indicate the hardware connections. The descriptions for all the symbols can be found in Table I (in Appendix).

management, seamless relocation of tasks, and continuous speed adjustment according to the latency overhead.

Outline: Section II describes the test environment, the controllers, and safety algorithms employed by the system. Section III describes different simplex strategies. Section IV illustrates how we can use available fog resources. In Section V, we design a monitor to observe the system operation which outputs a metric indicating if the car will remain in safe working region or not. Section VI reviews related work, and finally Section VII marks the conclusion. The main symbols used in the paper are described in the Table I.

II. DEEPNNCAR: TESTBED FOR AUTONOMOUS DRIVING

DeepNNCar¹ (in Figure 1) is built upon the chassis of Traxxas Slash 2WD 1/10 Scale RC car, which is similar to the

¹Build instructions, source code, datasets, and bill of materials for the DeepNNCar can be found at: <https://github.com/scope-lab-vu/deep-nn-car>

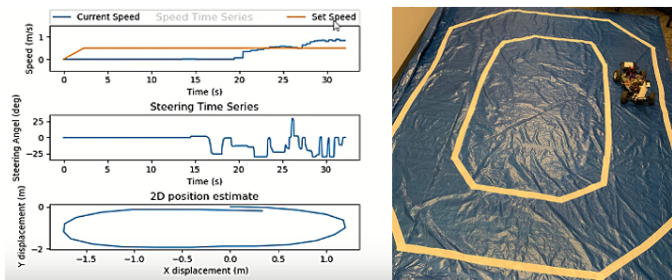


Fig. 3: (Left) shows different statistics of DeepNNCar: (1) current speed of the car, (2) predicted steering angle, and (3) a 2D trajectory of the car’s position on the track. (Right) shows the track testbed setup in our laboratory, which is the primary track on which we performed all of our experiments. Two other tracks with different shapes were also used during the experimentation.

ones used in F1/10 [17] racing competition. The RC car has two on-board motors, a servomotor for steering control, and a Titan 12T 550 motor for motive force, which are powered by a 8.4volts NiMH battery. Raspberry Pi 3 (RPi3) is the onboard computing unit, and it reserves two GPIO pins to generate Pulse Width Modulation (PWM) signals that are used to control the motors of the car. For the servomotor, a duty cycle range of (10, 20) corresponds to a continuous steering angle of $(-30^\circ, 30^\circ)$, and for the Titan 12T 550 motor, we operate within the PWM range of (15, 15.8), which corresponds to a vehicle speed range of (0, 1) m/s approximately. Figure 2 shows the data flow between different components, described in subsequent sections.

A. Sensors

A USB webcam is attached to the RPi3 to capture images at 30 FPS with a resolution of $320 \times 240 \times 3$ (320x240 RGB pixels). During autonomous driving, these images are used by the onboard controllers to compute desired steering angle. A slot-type IR opto-coupler speed sensor² is attached to the chassis near the rear wheel and counts revolutions of the wheel. The speed of the car is calculated based on the frequency of revolutions and is used to estimate the 2D relative position of the car (shown in Figure 3). During data collection camera images, vehicle speed, and steering angle are stored on-board the RPi3 onto a USB drive.

B. LEC in DeepNNCar

Perception based autonomous robots typically use either the classical mediated perception approach that performs separate perception-planning-control operations or an e2e learning approach which uses supervised learning to directly compute the control action. Recently, e2e learning has become appealing and widely used because of its conceptual simplicity and computationally efficient approach. It has been applied to different indoor and outdoor navigation tasks, such as obstacle avoidance [18], off-road autonomous navigation systems [19], and autonomous driving [2]. The e2e learning approach in fully autonomous cars was first demonstrated by ALVINN [2]

²We will abbreviate this sensor as opto-coupler in the text.

in 1989, and was recently extended by NVIDIA through their self-driving car, DAVE-II [1].

In the current implementation, the hardware uses e2e learning which implements a modified version of DAVE-II to predict steering (S_L). The original DAVE-II CNN [1] takes in image (I) as input and predicts S_L as the output without considering the impact of speed (V) on S_L . Our modified DAVE-II CNN has five convolutional layers and six fully connected layers. It takes in image (I) with resolution (66x200 RGB pixels) and vehicle speed (V) as inputs and predicts S_L as the output. The model is pre-trained with 6000 images collected from different tracks and lighting conditions.

The modification in the CNN model is required for two reasons. First, the steering and speed quantities are not decoupled, thus any change in the speed will impact the steering performance. We observed that the modified CNN takes wider trajectories at turns compared to the original one. Second, since the quality of the captured image deteriorates with increase in speed, additional information is required for the CNN to predict correct steering values.

C. Safety Supervisor

The Safety Supervisor is designed using classical image processing algorithms. It performs lane detection (LD), which involves detecting a lane against a dark surface. The LD algorithm is implemented in OpenCV and provides labelling information (straight, right, left, or out of track) for the track segment (\hat{M}) in which the car resides. The LD algorithm was tested using a dataset of 3000 images and it successfully labelled the track segments with an accuracy of 89.6%.

Lane Detection: The LD algorithm performs the following operations sequentially on a 200x66 gray scale image (to reduce the computation time).

- Gaussian blur and white masking: A 3x3 Gaussian kernel is convolved across the image to reduce the noise. Next, all pixels except those within a specified range (e.g., [215, 255]) are masked, thus differentiating the track lanes from the foreground.
- Canny edge detection: The algorithm first computes a gradient of pixel intensities. An upper and lower threshold of these gradients is defined at compile time. A comparison of the pixel gradients to these thresholds in addition to hysteresis (suppress all weak and unconnected edges) can determine if a pixel is an edge or not. The edges reveal the boundary of the lanes.
- Region of interest (ROI) selection: The image is divided into two similar 30x66 regions of interest to capture the left and right lane respectively.
- Hough line transform: A Hough line transform is applied to each ROI to detect the existence of a lane based on the results of the canny edge detection algorithm. Using this information we determine a label for the track segment.

For every estimate of the track segment (\hat{M}) we associate a discreet steering S_S : if LD detects the car in straight segment, $S_S = 0^\circ$; if LD detects the car in left segment, $S_S = -30^\circ$; and if LD detects the car in right segment, $S_S = 30^\circ$.

D. Simplex Architecture

The classical Simplex Architecture [12] has a complex controller (CC, LEC in our case) with high performance that is tested but unverified, an advanced controller (AC, Safety Supervisor) with high assurance to aid the LEC controller, and a decision manager (DM) which activates the AC whenever the CC is on the verge of jeopardizing the safety of the system. In the basic architecture we use Equation 1 to evaluate the steering S_{SA} of the Simplex Architecture:

$$S_{SA} = W_L \times S_L + W_S \times S_S \quad (1)$$

where $W_L, W_S \in \{0, 1\}$ and $W_L + W_S = 1$.

III. SIMPLEX STRATEGIES FOR DEEPNNCAR

In this section, we describe two simplex strategies that we have implemented and evaluated for the system. The first is based on the concept of arguing machines [15], while the second uses reinforcement learning.

A. Arguing Machine based Simplex approach (AM-Simplex)

The arguing machines [15] concept introduced by Fridman et al. involves two LECs working in parallel to predict the steering, and if the predicted steering values differ by more than a predefined threshold, then the control is given to a human driver. In our approach of AM-Simplex, we use the LEC and safety supervisor as the two controllers, and if the difference between their predicted steering values is higher than a predefined threshold, then the steering is computed by Equation 2 instead of a human driver. However, if the difference between the predicted steering values are lower than the threshold, then the LEC action is chosen to drive the system.

$$S_{AM} = 0.8 \times S_L + 0.2 \times S_S \quad (2)$$

The arbitration weights (W_L, W_S) are fixed (see Equation 2) and were found through trial and error experimental runs.

The speed of the system is varied depending on the state of AM-Simplex. If there are no disagreements between the controllers' predicted steering values, then the speed is continuously increased to optimize the systems performance. However, if there are continuous disagreements, then the speed is reduced.

Several parameters like the predefined threshold, arbitration weights (W_L, W_S), and the change in speed (δV) are track specific and configuring them requires a number of experimental runs and human labor. In order to overcome the arbitrary parameter selection process, we use an RL approach for the arbitration logic.

B. Reinforcement Learning based Simplex (RL-Simplex)

The training of an autonomous system is typically modeled using a Markov decision process (MDP) [20], which can be represented by four elements: state (S), action (a), transition probability ($P(R_2|R_1, a)$), and a reward function ($r(R_2|R_1, a)$). The goal of reinforcement learning is to find a policy or a list of actions to take for various states in

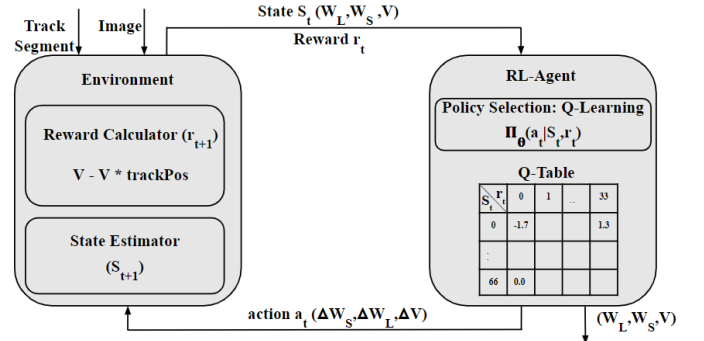


Fig. 4: Agent-Environment interactions in the RL actor (Figure 2) of DeepN-NCar.

the environment that maximizes the reward function. RL is a framework that enables the learning of a policy in a MDP when the transition probabilities and the reward functions are unknown [4]. When those quantities are known, techniques such as dynamic programming can be used to learn the policy function. In such cases, policy learning can be performed offline. However, RL must be performed online meaning the actions are not pre-determined as in an offline analysis.

There are two main learning strategies in reinforcement learning (1) model-based learning and (2) model-free learning. Model-based learning involves consideration of empirical models for the transition probabilities and the reward function, and the use of simulations or experimental data to learn parameters of interest. As more data is available, the learned parameters can be updated using algorithms, such as stochastic gradient search. Model-free learning does not consider any empirical models but learns the transition probabilities and reward function directly from data [21]. In this work, we use the model-free Q-learning [22] approach to arbitrate the decision manager logic.

The **RL-Manager** involves different components of DeepN-NCar which are responsible for the Q-learning process. The interface (see Figure 4) shows the different messages that are being published and consumed by each component (RL-Agent, Environment).

The **Environment** component within the RL-Manager tracks and estimates the state (S) of the system based on an internal estimate of the MDP and computes a reward (r) for an action (a).

The State (S) represents the current situation of the RL-agent in the environment. These states continuously change as the agent interacts with the environment, and the state information is used by the agent to continuously learn the optimal action. The goal of RL is to find the optimal arbitration weights (W_L, W_S) (see Equation 1) and speed (V) that are encoded as the state information $S(W_L, W_S, V)$. It is important to have discretized states to build the MDP and perform the necessary action. For each of the state variable $W_L, W_S \in (0, 1)$ and $V \in (15.58, 15.62)(PMM)$, we define a set of equidistant points of separation $\delta W_L, \delta W_S = 0.05$ and $\delta V = 0.01$ to get a vector of arbitration weights containing 21 elements and a vector of V containing 41 elements.

action space	$\uparrow V$ by 0.01	$\downarrow V$ by 0.01	NOP
$\uparrow W_L$ by 0.05	(0.55,0.45,15.86)	(0.55,0.45,15.84)	(0.55,0.45,15.85)
$\downarrow W_L$ by 0.05	(0.45,0.55,15.86)	(0.45,0.55,15.84)	(0.45,0.55,15.85)
NOP	(0.50,0.50,15.86)	(0.50,0.50,15.84)	(0.50,0.50,15.85)

TABLE II: Action space for a given state ($W_L = 0.5$, $W_S = 0.5$, $V = 15.85$). Similar action combinations are generated for other states. NOP: means no operation

The second task of the environment component is to compute a reward for the previous action performed by the agent. The reward is formulated to account for V and \hat{M} , $r(s_t, a_t) = V_t - V_t \cdot \hat{t}$, where V_t is the speed of the car in the current state and \hat{t} is a scalar quantity computed based on the deviation of the car from the center of the track. The measure \hat{t} is decided by the LD algorithm of the safety supervisor: if the algorithm detects both lanes of the track in the captured image, then the car is at the center of the track ($\hat{t} = 0$); if the LD algorithm detects only one lane, then the car has slightly deviated from the center ($\hat{t} = 1/2$); and if it detects no lanes then the car is out of track ($\hat{t} = 10$). The system may initially stray away from the center of the track or choose to remain at low speeds; however as it goes on receiving lower rewards it learns to optimize its speed while also trying to keep the center of the track in an effort to receive the highest reward.

RL-agent selects optimal actions for the state information provided by the environment. For each state $s \in S$, the agent performs an action $a \in A$, which results in a reward, $r : S \times A \rightarrow \mathbb{R}$, as the agent transitions to state $s' \in S$. The possible action space for a state with ($W_L = 0.5$, $W_S = 0.5$, $V = 15.85$) is shown in Table II, and a similar action space is created for all the different combinations of (W_L, W_S, V). Thus, there are 9 possible actions that can be performed in any state.

For each state-action pair (s, a) , the agent learns the “quality” $Q(s, a)$ of taking action a in state s . This quality $Q(s, a)$ is defined as the expected value of the immediate reward for taking action a in state s plus the maximum attainable future reward (with temporal discounting) from the next state s' . During training, after taking action a_t in state s_t , the agent updates the quality estimate $Q(s_t, a_t)$ based on the observed immediate reward $r(s_t, a_t)$ and based on the estimated attainable reward from the next state s_{t+1} . We can estimate attainable reward in state s_{t+1} as $\max_{a \in A} Q(s_{t+1}, a)$.

The Q value is updated using the Bellman equation, which takes the current state and action as inputs along with the parameters $\alpha \in [0, 1]$ and $\gamma \in [0, 1]$. Parameter α controls the learning rate of the algorithm, while parameter γ represents the discount factor which balances the importance of future benefits over immediate benefits (i.e., decreasing γ increases priority on obtaining immediate rewards).

$$Q_{new}(s_t, a_t) = Q(s_t, a_t) + \alpha [r(s_t, a_t) + \gamma \cdot \max_{a \in A} Q(s_{t+1}, a) - Q(s_t, a_t)] \quad (3)$$

The Q values computed by the Q-learning algorithm are stored in a Q-Table, which is a lookup table that stores for each state-action pair the Q value $Q(s, a)$ and the immediate reward $r(s, a)$.

C. System Integration

The components of DeepNNCar and the data flow among them is shown in Figure 2. DeepNNCar uses ZeroMQ (ZMQ) for communication among its components. The camera provides new images at 30 Hz and the IR opto-coupler speed sensor continuously collects data to compute the speed of the car. Then, the camera device actor³ and the opto-coupler device actor periodically publish the images (I) and speed (V) to all the subscriber components. However, the LEC actor, the safety supervisor actor, and the RL-Actor are aperiodic consumers (see [24]) which do not consume the sensor values until prompted by the DMA. The interaction between the periodic publishers and aperiodic consumers is handled with the help of a Message Buffer Actor (MBA), which has a one buffer queue to store the published data (both I and V) along with a sequence label. The data in the MBA gets updated according to the sampling period of the sensors. However, this data cannot be published until the MBA has received a sampling tick and a request from the DMA to publish the data of a certain label. Once the MBA receives this request, it publishes the I and V messages to all subscribed components. Using this data, the LEC actor predicts S_L , the Safety Supervisor computes S_S , track position \hat{M} , and $STOP$ (a command issued if the car goes out of the track), and the RL-Actor computes W_L , W_S and V_{SET} using Q-learning.

Decision manager Actor: The DMA issues requests for the sequence label and data S_L , S_S from the controllers, and for W_L , W_S , and V_{SET} from the RL actor. Once the controller and the RL actor have finished computing, they reply to the DMA their label and values. The DMA then matches the labels and computes S_R using Equation 1 before feeding S_R and V_{SET} to the GPIO device actor, which controls the two motors. After applying the controls to GPIO, the DMA starts a new cycle. This cycle continuous indefinitely until it is terminated by the STOP signal from the Safety Supervisor or manually by the user. The tasks performed between two sampling ticks of the DMA is one control cycle of the system and the time taken to perform one control cycle is referred to as the inference pipeline time T_R . The T_R varies for every control cycle, but the average inference time for RL-Simplex is experimentally found to be 130ms (see Figure 6).

Other than computing S_R , the DMA can also actively switch among the different controllers (LEC, Safety Supervisor) and the different simplex strategies (AM-Simplex, RL-Simplex). During an initial exploration of an unknown track, the DMA selects the AM-Simplex to familiarize and learn the different track segments. Once it gathers enough data, the DMA switches to the RL-Simplex to explore and learn the Q-Table of optimal arbitration weights (W_L , W_S) and speed (V_{SET}), which is used during testing (exploitation).

D. Experiments

To get a Q-Table of the state-action-rewards for the RL-Simplex, we performed an exploration of 1000 steps on the

³A device actor converts hardware sensor information into topics that can be published and subscribed to, see [23].

track shown in Figure 3. Continuous exploitation-exploration scheme was employed to evaluate the learning and fix the number of exploration steps. We also tested RL-Simplex by running the car in exploitation mode on two other tracks which had different shapes and geometric turns.

Experiment 1: Comparing safety violations of different strategies: In our experiments, a safety violation refers to the number of times the car exits the track boundaries. We evaluated the number of safety violations performed by the different strategies (see Figure 5). All the trial runs were performed on the track in Figure 3 for 10 laps. For the safety supervisor and LEC, each trial run maintained a constant vehicle speed (ranging from 0.25 to 0.65 m/s) using a PID controller and the number of safety violations were recorded. The AM-Simplex and RL-Simplex strategies do not maintain a constant speed. Therefore, the safety violations for these strategies were segregated into different speed groups after completing the experiments. The RL-Simplex was found to perform most reliably with the lowest number of violations.

Experiment 2: Comparing inference times and maximum operable speeds of different strategies: Figure 6 illustrates the inference times of the different controllers and strategies. We observe that the safety supervisor and LEC have lower pipeline times (80 ms) while the AM-Simplex and RL-Simplex controllers have a higher pipeline time (130 ms) due to the increased computation of the Simplex Architecture.

We also recorded the maximum operable speed for the different strategies (Figure 7). The safety supervisor and LEC have a similar speed pattern due to the PID controller they use. However, for AM-Simplex and RL-Simplex the speeds are continuously updated depending on the mode of the track. It can be seen that RL-Simplex optimizes the speed of the car better compared to the other strategies.

IV. INTEGRATING FOG COMPUTING

DeepNNCar runs with a miniature computing unit (RPi3), which must support multiple sensors (camera, opto-coupler) and perform expensive deep learning and image processing computations. This constant workload will increase the power consumption, CPU utilization and the temperature of RPi3 beyond 70°C (configured soft limit). Beyond the soft limit,

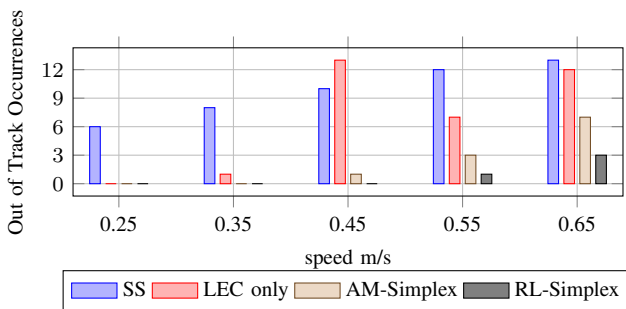


Fig. 5: The DeepNNCar performs fewer safety violations when combined with the RL-Simplex strategy. (a) SS: driving only with the OpenCV safety supervisor code, (b) LEC: driving only with the modified Dave-II model, (c) AM-Simplex, and (d) RL-Simplex. The horizontal axis shows the different speeds of the car during the experiment.

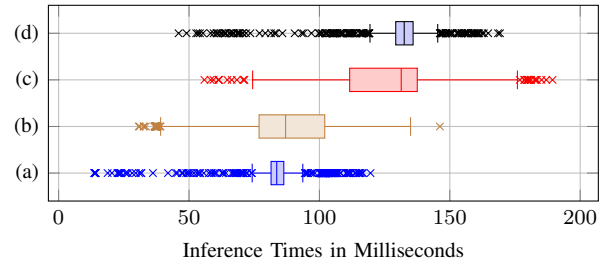


Fig. 6: Inference times in milliseconds of (a) Safety Supervisor: driving only with the OpenCV safety supervisor code, (b) LEC: driving only with the modified Dave-II model, (c) AM-Simplex, and (d) RL-Simplex

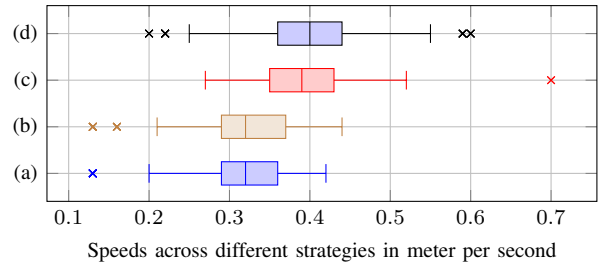


Fig. 7: Speeds in meter per second of (a) Safety Supervisor: Driving only with the OpenCV safety supervisor code, (b) LEC: Driving only with the modified Dave-II model, (c) AM-Simplex, and (d) RL-Simplex

the clock speed and the operating voltage of RPi3 is reduced [25]. A simple approach to address the increasing temperature and CPU utilization problem would be to add multiple computing devices on-board the DeepNNCar and distribute the tasks among them. However, this approach requires additional external power sources, which increases development cost of the platform. Alternatively, since the RPi3 supports WiFi connectivity, we can setup wireless communication with other cars or fog nodes using ZMQ and offload some non-critical tasks. We use the second approach to utilize the wireless communication feature of the framework, and also keep the costs of the platform low. However, we offload only non-critical tasks (like RL-Manager, which only has to access the Q-Table and fetch actions), and no critical components like Safety Supervisor or Decision Manager will be offloaded.

To manage the offload challenges, the middleware framework has a Resource Manager (RM) that performs the following tasks: (1) continuous monitoring of resource state (temperature and CPU Utilization), (2) selection of an optimal fog node for task deployment, and (3) readjusting the vehicle speed (V) according to variations in the the inference pipeline times. The RM continuously monitors the temperature and CPU utilization of the on-board computer and may offload one or more tasks to the other fog nodes if necessary.

In the background, the RM continuously performs a latency test every 30 seconds using the iPerf [26] networking tool to select a fog node with lowest latency (as it increases the inference time T_R). If the temperature exceeds 70°C, the RM stops the tasks on RPi3 and seamlessly connects to identical tasks running on the selected fog nodes using ZMQ. Once the temperature has fallen below the threshold (70°C), the RM reactivates the tasks on the RPi3.

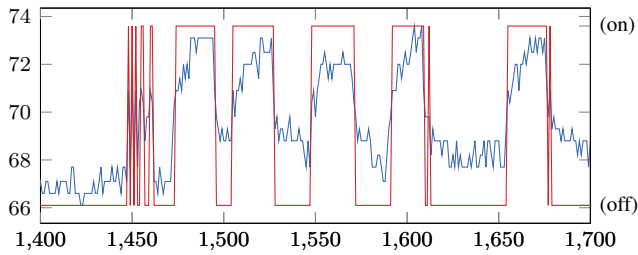


Fig. 8: The effect of offloading the tasks in response to high temperature per iteration of the inference pipeline. The trigger to offload the task is 70°C. The blue line shows the temperature in Celsius. The red line shows when the tasks were offloaded to the fog (on=on fog, off=off fog). The graph shows a subset of iterations (total 10000 iterations).

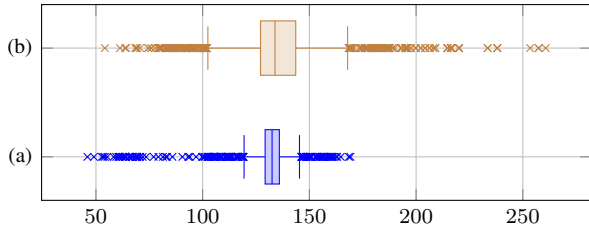


Fig. 9: Inference times in milliseconds (a) RL-Simplex with all tasks executed onboard (b) RL-Simplex with RL-Manager offloaded.

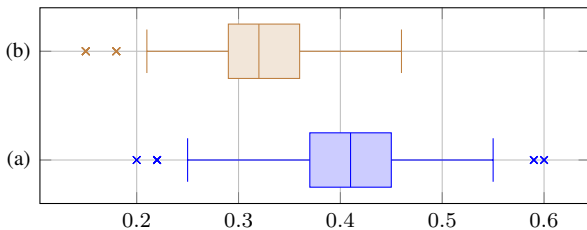


Fig. 10: Speed readjustment during offload (m/s) (a) RL-Simplex with all tasks executed onboard (b) RL-Simplex with RL-Manager offloaded.

Figure 9 shows an increase in the pipeline times (due to network latency) during task offload. In order to compensate for the increased time, the RM instructs the DM to saturate (limit) the top speed of the car. The saturated maximum speed V_{MAX} is calculated using the safe distance (d_S) which is the closest distance to the track turns at which the car will have to take a decision to avoid going off the track. The d_S is a track specific quantity which was found to be 0.09m for our track (see Figure 3). Therefore, any decision taken before reaching this distance will give the car a good turning radius. However, any decision taken after this distance will leave the car with insufficient space to turn which will result in a safety violation. V_{MAX} is computed as: $V_{MAX} = \frac{d_S}{T_R}$, where T_R is the inference pipeline time (discussed in section III-C). During task offloads, the DMA has to wait longer for a reply from the offloaded component due to the latency overhead, which increases the T_R .

A. Experiments

For the task offloading experiments, we had a wireless reply-request communication between the onboard RPi3, a dell laptop (with intel 4-core processor) and a desktop (with 32 AMD Ryzen Threadripper 16-core processor). These exper-

imental results were collected in real-time when the system was running.

Experiment 3: Temperature mitigation: Figure 8 shows the temperature of the RPi3 to drop below the threshold (70°C) when the tasks are offloaded to a fog device. It also shows that the tasks were got back to RPi3 once the temperature dropped below the threshold.

Experiment 4: Increased inference time and Decreased speed: Figure 9 shows the RL-Simplex with all tasks performed onboard RPi3 to have lower inference time T_R compared to the RL-Simplex with RL-Manager offloaded to a fog node. Figure 10 shows that the DeepNNCar with offloaded RL-Manager runs at lower (safe) speeds in order to compensate for the increased inference time T_R .

V. SYSTEM LEVEL CONFIDENCE ESTIMATION

For most autonomous systems, it is necessary to develop a mechanism that can monitor the system operation and provide a level of confidence as to how safe the system will be in different operating scenarios. This is a difficult task because it requires an effective knowledge of the distribution of the environment in which the system operates. In a limited setting where the systems operation and the environment modes can be characterized we can use a Bayesian network to learn the probability distribution. We then can use this distribution to estimate the probability that the system will remain safe given a particular control action. The evidence for the confidence increases over time as we collect more data from safe operation trajectories.

In case of the DeepNNCar, we use a Bayesian Network model (Figure 11) to estimate the probability that the car will remain on track, given its current state and control actions. Data collected during training and evaluation, is used to build a model to estimate the current position of the car, using the output of the IR opto-coupler and the steering commands issued to the car. The data is also used to identify safe-turn regions (in different segments of the track) and the ranges for commands that keep the car within the track (at different speeds of operation). The nodes *current-position*, *current-velocity* and *current-steering* capture the current state of the car. The node *SafeTurnRegion* captures the likelihood of the car being in the safe-turn region when a control-cycle update is triggered. *SafeTurnRegion* and the steering command *CmdSteeringOnTurn* issued when the car is in the safe turn region influence the likelihood of the car remaining on track (*InTrack*). It is important to note that this network focuses on the performance of the overall system and does not monitor and/or assess the performance of individual components (sensors, actuators, Safety Supervisor, LEC or the RL-Manager) and their contributions to the performance of the system.

The *current-position* node corresponds to the car distance from the next safe turn region. The discrete states based on the distance include *On*, *Near* and *Far*. The discrete states for *current-velocity* are *Slow* (less than 0.25 m/s), *Medium* (between 0.25 and 0.6 m/s) and *Fast* (greater than 0.6 m/s). The *current-steering* node corresponds to the current steering

TABLE III: Conditional Probability Table for *SafeTurnRegion* node.

Current Position	Near									On									Far											
Current Velocity	Slow			Medium			Fast			Slow			Medium			Fast			Slow			Medium			Fast					
Current Steering*	S	L	R	S	L	R	S	L	R	S	L	R	S	L	R	S	L	R	S	L	R	S	L	R	S	L	R			
SafeTurnRegion =Yes	1	0.8	0.8	0.9	0.6	0.6	0.2	0.1	0.1	1	1	1	1	1	1	1	1	1	1	1	1	0.9	0.9	0.9	0.8	0.7	0.7	0.5	0.2	0.2
SafeTurnRegion =No	0	0.2	0.2	0.1	0.4	0.4	0.8	0.9	0.9	0	0	0	0	0	0	0	0	0	0	0	0	0.1	0.1	0.1	0.2	0.3	0.3	0.5	0.8	0.8

* - Current Steering states : S=Strait, L=Left, R=Right.

TABLE IV: Conditional Probability Table for *InTrack* node

SafeTurnRegion	Yes									No								
CmdSteering	Left			Strait			Right			Left			Strait			Right		
Velocity	Slow	Med.	Fast	Slow	Med.	Fast	Slow	Med.	Fast	Slow	Med.	Fast	Slow	Med.	Fast	Slow	Med.	Fast
InTrack=Y	0.6	0.2	0	0.7	0.5	0	1	0.9	0	0.2	0.1	0	0.3	0.2	0	0.5	0.4	0
InTrack=N	0.4	0.8	1	0.3	0.5	1	0	0.1	1	0.8	0.9	1	0.7	0.8	1	0.5	0.6	1

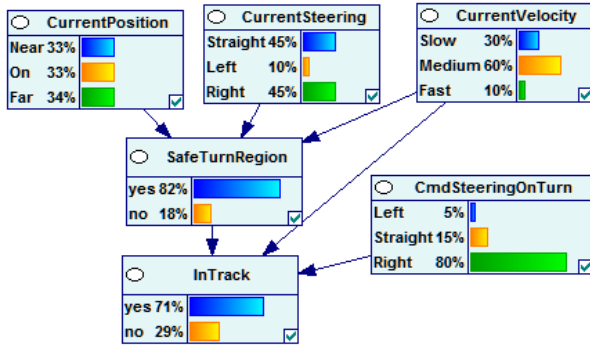


Fig. 11: Bayesian Network model for Safety Assurance. Tables III and IV capture the conditional probability tables for the nodes *SafeTurnRegion* and *InTrack* respectively.

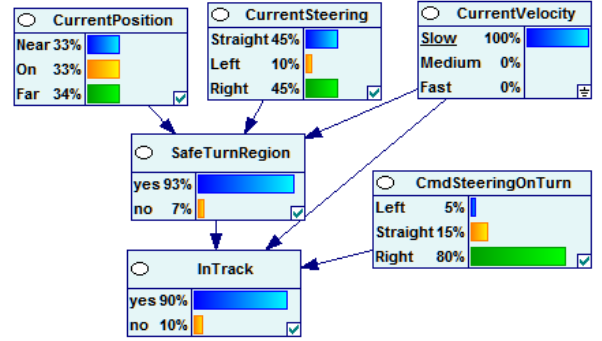


Fig. 12: Bayesian Inference when *current-velocity* is set to *Slow*

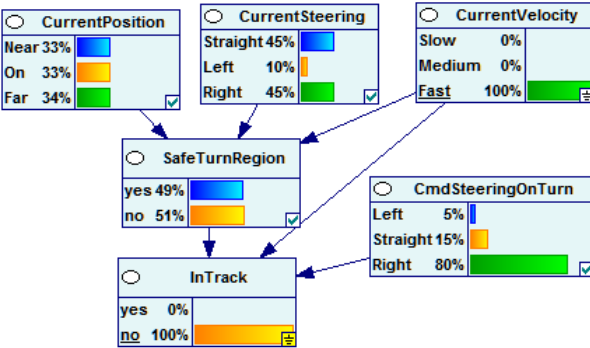


Fig. 13: Bayesian Inference when *current-velocity* is set to *Fast*

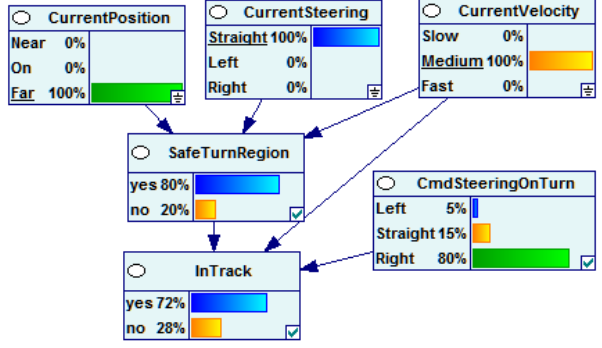


Fig. 14: Bayesian Inference when *current-velocity* is set to *Medium*, *current-steering* is set to *Strait* and *current-position* is set to *Far*

angle of the car relative to its desired direction and includes the states *left* (less than -10°), *strait* (between -10° and $+10^\circ$) and *right* (greater than 10°). The node *CmdSteeringOnTurn* corresponds to the steering command issued when the car is on the safe turn region and includes the states (*Left*, *Right* and *Strait*) which are based on the range of the steering command values.

SafeTurnRegion indicates if the car will be in the safe turn region when a control command is executed. The node *InTrack* indicates if the car will remain on track when the turn is executed. Both these nodes include two states *yes* and *no*.

The priors and the conditional probability tables have been filled based on our understanding of the system during ex-

perimentation. The bar graph in each of the root nodes in Figure 11 shows the node probabilities based on logical inferences using the priors and conditional probabilities. Tables III and IV capture the conditional probability tables for the nodes *SafeTurnRegion* and *InTrack* respectively.

The prior probabilities on the *Current-Position* node shows that there is an equal chance of the car being in the three position states. With regards to *Current-Steering*, the *Left* state is observed only when there is an error or there is a course correction for an error. The *Current-Velocity* has been observed to be in the medium range most of the time giving the *Medium* state a higher prior

probability. The lower velocity states are observed during start up phases, while the fast speeds are not so commonly seen. Given the shape of the track, the steering command during turns is mostly right and hardly left as seen in the priors for *CmdSteeringOnTurn*.

Based on the priors for the root (observation) nodes and the likelihoods captured in the conditional probability tables (Tables III, IV), the priors for the assurance nodes (*SafeTurn-Region* and *InTrack*) can be inferred. The prior probability of being on track (0.7) reflects our experimental evidence with RL-simplex architecture. The Bayesian network model was used to compute the assurance metrics (the probability of car being on the track and the probability of car being in the turn region to execute control action) under different situations. This was done by setting the evidence on the root (observation) nodes and executing the Bayesian inference engine to compute the posterior probabilities.

The model predicts that when the *current-velocity* is set to *Slow*, there is a high probability of the car being in the safe turn region and remaining on the track (Figure 12). Alternately, figure 13, shows that when the speed is set to *Fast*, the chance of being in the safe turn region to execute a control action is greatly reduced and there is no chance of remaining on the track. Figure 14 shows that when the *current-velocity* is *Medium*, *current-steering* is *Straight* and the *current-position* is *Far* from the safe turn region, there is a good chance of the car executing a control action in the safe turn region (80%) and remaining on track (77%).

The results of the Bayesian Network show a trend that agrees with our experimental observations. We are exploring the possibility of using a continuous Bayesian network model to predict these performance metrics.

VI. RELATED WORK

Our work encompasses several topics including Autonomous system testbeds and Simplex Architectures. These topics are briefly discussed below.

Autonomous testbeds: There have been several ongoing projects related to physical testbeds for autonomous systems. F1/10 [17] is an autonomous racing competition with cars built on Traxxas 1/10 scale RC car (like DeepNNCar) with an expensive NVIDIA’s Jetson TX1 onboard computing unit. These autonomous builds use cameras, IMUs, and expensive LIDAR (\$1,775) systems for performing simultaneous localization and mapping (SLAM). An F1/10 car is far more expensive compared to the cost of DeepNNCar (approx. \$3000 vs. \$418). DeepPicar [6] is another platform which is built using a smaller 1/24 scale RC chassis. This platform also uses an RPi3 as the computing unit and performs autonomous driving using NVIDIA’s DAVE-II CNN. This build is relatively inexpensive (\$70), but has a considerably smaller chassis and uses discrete steering actuation unlike DeepNNCar which performs continuous steering.

Simplex architectures and arbitration logic: Simplex Architectures [12], [14] have been extensively used in CPS to provide safety guarantees to control systems. They have been

used in different systems including online control systems [27], real time embedded systems [28], and unmanned aerial vehicles (UAV) [13]. Like simplex architectures, Run Time assurance (RTA) frameworks [29] ensure the safety of the system by adding simple baseline controllers in parallel to unverified complex controllers. These implementations use arbitration logic to switch between the controllers. The two widely used switching criteria are linear matrix reachability [30] and hybrid system reachability [31]. None of the above discussed architectures or switching criteria considers the use of context and modes of the working environment in determining the arbitration weights. Using RL, we were able to determine mode specific weights for the arbitration logic. In addition, these switching criteria could be slow due to the state explosion problem in reachability analysis. However, RL-Simplex can perform the required computations within 20 milliseconds.

Safety via contracts: Andalam, Sidharta, et al. [32] have discussed CLAIR, a contract-based framework for developing resilient CPS architectures. This work is predominantly a contract-based framework for components in different levels of abstraction. Formal contracts are used to capture the assumptions about the environment and guarantees provided by the systems components. It also employs resilience managers at the component level and the layer level to monitor the safety contracts. "Safety via Contracts" is the underlying idea behind this framework. If the A-G contract fails then the component/system violates the safety. Instead of using contracts for safety guarantees, our approach uses the simplex architecture approach (discussed in section II) where verifying the safety supervisor and the decision manager is sufficient to prove the safety of the composite system.

Phan, Dung et al. [14] have integrated Simplex Architecture with A-G contracts (to determine the switching logic), and have named it as Component Based Simplex Architecture (CBSA). In addition to the switching logic, A-G contracts are also used to provide a run-time assurance for the systems safety using the components assured contracts. While CBSA uses A-G contracts for the arbitration logic and run-time assurances, our approach uses RL for the arbitration logic. We then use the current state of the car information to build a Bayesian Network model to monitor the system’s operation and provide an estimate of its overall confidence.

VII. CONCLUSION AND FUTURE WORK

In this work, we have introduced a middleware framework to improve the performance and safety guarantees of autonomous robots using LECs. We have discussed the problems associated with the LECs and have further implemented it on our physical test-bed, DeepNNCar. To improve the safety guarantees of the system, our framework allows for the integration of safety supervisors, and composition of Simplex Architectures. Furthermore, we have also implemented two simplex strategies (AM-Simplex, RL-Simplex) and evaluated their effects on speed, steering, and safety performance. Our analysis of the results shows that the RL-Simplex outperforms the other

implementations with the fewest safety violations and maximal safe operating speed of the car.

The framework also has a system monitor which estimates a confidence metric, that indicates the likelihood of the car operating in a safe region of the track. The results of the monitor are in complement with our observed results. Furthermore, we have discussed the ability of DeepNNCar to dynamically offload tasks and adjust the vehicle speed according to the latency overhead.

This framework has potential applications in factory and warehouse robots which primarily perform unloading and delivery of goods from one location to another. In such scenarios, our framework could allow multiple robots to communicate among them to perform a coordinated task, and aid in safe navigation.

In future, we plan to include multiple cameras and Lidar on DeepNNCar to perform indoor localization and mapping. For the framework, we plan to integrate an online confidence estimation system which uses real time data to predict the confidence metric.

Acknowledgements: This work was supported by the DARPA and Air Force Research Laboratory. Any opinions, findings, and conclusions or recommendations expressed in this material are those of the author(s) and do not necessarily reflect the views of DARPA or AFRL.

REFERENCES

- [1] M. Bojarski, D. Del Testa, D. Dworakowski, B. Firner, B. Flepp, P. Goyal, L. D. Jackel, M. Monfort, U. Muller, J. Zhang et al., "End to end learning for self-driving cars," *arXiv preprint arXiv:1604.07316*, 2016.
- [2] D. A. Pomerleau, "ALVINN: An autonomous land vehicle in a neural network," in *Advances in neural information processing systems*, 1989, pp. 305–313.
- [3] L. Apvrille, T. Tanzi, and J.-L. Dugelay, "Autonomous drones for assisting rescue services within the context of natural disasters," in *General Assembly and Scientific Symposium (URSI GASS), 2014 XXXIth URSI*. IEEE, 2014, pp. 1–4.
- [4] L. P. Kaelbling, M. L. Littman, and A. W. Moore, "Reinforcement learning: A survey," *Journal of artificial intelligence research*, vol. 4, pp. 237–285, 1996.
- [5] D. Silver, J. Schrittwieser, K. Simonyan, I. Antonoglou, A. Huang, A. Guez, T. Hubert, L. Baker, M. Lai, A. Bolton et al., "Mastering the game of go without human knowledge," *Nature*, vol. 550, no. 7676, p. 354, 2017.
- [6] M. G. Bechtel, E. McElhiney, and H. Yun, "DeepPicar: A low-cost deep neural network-based autonomous car," *arXiv preprint arXiv:1712.08644*, 2017.
- [7] Y. Tian, K. Pei, S. Jana, and B. Ray, "DeepTest: Automated testing of deep-neural-network-driven autonomous cars," in *Proceedings of the 40th International Conference on Software Engineering*. ACM, 2018, pp. 303–314.
- [8] K. Pei, Y. Cao, J. Yang, and S. Jana, "DeepXplore: Automated whitebox testing of deep learning systems," in *Proceedings of the 26th Symposium on Operating Systems Principles*. ACM, 2017, pp. 1–18.
- [9] X. Huang, M. Kwiatkowska, S. Wang, and M. Wu, "Safety verification of deep neural networks," in *International Conference on Computer Aided Verification*. Springer, 2017, pp. 3–29.
- [10] W. Xiang, H.-D. Tran, and T. T. Johnson, "Reachable set computation and safety verification for neural networks with ReLU activations," *arXiv preprint arXiv:1712.08163*, 2017.
- [11] C. Richter, W. Vega-Brown, and N. Roy, "Bayesian learning for safe high-speed navigation in unknown environments," in *Robotics Research*. Springer, 2018, pp. 325–341.
- [12] L. Sha, "Using simplicity to control complexity," *IEEE Software*, no. 4, pp. 20–28, 2001.
- [13] P. Vivekanandan, G. Garcia, H. Yun, and S. Keshmiri, "A simplex architecture for intelligent and safe unmanned aerial vehicles," in *2016 IEEE 22nd International Conference on Embedded and Real-Time Computing Systems and Applications (RTCSA)*. IEEE, 2016, pp. 69–75.
- [14] D. Phan, J. Yang, M. Clark, R. Grosu, J. D. Schierman, S. A. Smolka, and S. D. Stoller, "A component-based simplex architecture for high-assurance cyber-physical systems," in *17th International Conference on Application of Concurrency to System Design, ACSD 2017, Zaragoza, Spain, June 25-30, 2017*, 2017, pp. 49–58. [Online]. Available: <https://doi.org/10.1109/ACSD.2017.23>
- [15] L. Fridman, B. Jenik, and B. Reimer, "Arguing machines: Perception-control system redundancy and edge case discovery in real-world autonomous driving," *arXiv preprint arXiv:1710.04459*, 2017.
- [16] G. Biswas, H. Khorasgani, G. Stanje, A. Dubey, S. Deb, and S. Ghoshal, "An approach to mode and anomaly detection with spacecraft telemetry data," *International Journal of Prognostics and Health Management*, 2016.
- [17] "F1Tenth autonomous racing competition." [Online]. Available: [\url{http://f1tenth.org/}](http://f1tenth.org/)
- [18] U. Muller, J. Ben, E. Cosatto, B. Flepp, and Y. L. Cun, "Off-road obstacle avoidance through end-to-end learning," in *Advances in neural information processing systems*, 2006, pp. 739–746.
- [19] M. Bajracharya, A. Howard, L. H. Matthies, B. Tang, and M. Turmon, "Autonomous off-road navigation with end-to-end learning for the LAGR program," *Journal of Field Robotics*, vol. 26, no. 1, pp. 3–25, 2009.
- [20] M. L. Puterman, *Markov decision processes: discrete stochastic dynamic programming*. John Wiley & Sons, 2014.
- [21] J. Kober and J. Peters, "Reinforcement learning in robotics: A survey," in *Reinforcement Learning*. Springer, 2012, pp. 579–610.
- [22] C. J. Watkins and P. Dayan, "Q-learning," *Machine learning*, vol. 8, no. 3–4, pp. 279–292, 1992.
- [23] A. Dubey, G. Karsai, P. Volgyesi, M. Metelko, I. Madari, H. Tu, Y. Du, and S. Lukic, "Device access abstractions for resilient information architecture platform for smart grid," *IEEE Embedded Systems Letters*, pp. 1–1, 2018.
- [24] N. Mahadevan, A. Dubey, and G. Karsai, "Model-based software health management for real-time systems," in *IEEE Aerospace Conference(AERO)*, vol. 00, 03 2011, pp. 1–18. [Online]. Available: doi.ieeecomputersociety.org/10.1109/AERO.2011.5747559
- [25] "Raspberry Pi frequency management." [Online]. Available: <https://www.raspberrypi.org/documentation/hardware/raspberrypi/frequency-management.md>
- [26] "iPerf: A tool for measuring network performance." [Online]. Available: <https://iperf.fr/>
- [27] D. Seto and L. Sha, "A case study on analytical analysis of the inverted pendulum real-time control system," *CARNEGIE-MELLON UNIV PITTSBURGH PA SOFTWARE ENGINEERING INST, Tech. Rep.*, 1999.
- [28] S. Bak, D. K. Chivukula, O. Adekunle, M. Sun, M. Caccamo, and L. Sha, "The system-level simplex architecture for improved real-time embedded system safety," in *Real-Time and Embedded Technology and Applications Symposium, 2009. RTAS 2009. 15th IEEE*. IEEE, 2009, pp. 99–107.
- [29] M. Clark, X. Koutsoukos, J. Porter, R. Kumar, G. Pappas, O. Sokolsky, I. Lee, and L. Pike, "A study on run time assurance for complex cyber physical systems," *AIR FORCE RESEARCH LAB WRIGHT-PATTERSON AFB OH AEROSPACE SYSTEMS DIR, Tech. Rep.*, 2013.
- [30] D. Seto, B. Krogh, L. Sha, and A. Chutinan, "The simplex architecture for safe on-line control system upgrades," in *Proceedings of the American Control Conference*, vol. 6. AMERICAN AUTOMATIC CONTROL COUNCIL, 1998, pp. 3504–3508.
- [31] S. Bak, K. Manamcheri, S. Mitra, and M. Caccamo, "Sandboxing controllers for cyber-physical systems," in *Cyber-Physical Systems (ICPS), 2011 IEEE/ACM International Conference on*. IEEE, 2011, pp. 3–12.
- [32] S. Andalam, D. J. X. Ng, A. Easwaran, and K. Thangamariappan, "Clair: A contract-based framework for developing resilient cps architectures," in *2018 IEEE 21st International Symposium on Real-Time Distributed Computing (ISORC)*. IEEE, 2018, pp. 33–41.